PCCP

On the use of thioamides as fluorescence quenching probes for tracking protein folding and stability

Journal:	*Physical Chemistry Chemical Physics*
Manuscript ID:	CP-PER-12-2013-055525.R1
Article Type:	Perspective
Date Submitted by the Author:	26-Feb-2014

Complete List of Authors:	Petersson, E. James; University of Pennsylvania, Chemistry Goldberg, Jacob; University of Pennsylvania, Chemistry Wissner, Rebecca; University of Pennsylvania, Chemistry

Cite this: DOI: 10.1039/c0xx00000x

www.rsc.org/pccp

PERSPECTIVE

On the use of thioamides as fluorescence quenching probes for tracking protein folding and stability

E. James Petersson,* Jacob M. Goldberg, and Rebecca F. Wissner

Received (in XXX, XXX) Xth XXXXXXXXX 20XX, Accepted Xth XXXXXXXXX 20XX

DOI: 10.1039/b000000x

Our laboratory has developed thioamide analogs of the natural amino acids as minimally-perturbing fluorescence quenching probes that can be placed at many locations in a protein sequence. We have shown that the mechanism of quenching can be either Förster resonance energy transfer (FRET) or photoinduced electron transfer (PET), depending on the identity of the donor fluorophore. Furthermore, we have shown that one can use a combination of semi-synthetic methods to label full-sized proteins with fluorophore/thioamide pairs. These probes can be used to probe protein/protein interactions, protein folding or misfolding, and proteolysis.

1. Introduction

One of the fundamental challenges of Biochemistry is to understand the folding and conformational rearrangements of proteins, which result from the complex, dynamic interplay of a large number of non-covalent interactions of little individual consequence. Many proteins require dramatic structural rearrangements for function, even relatively small proteins such as 148 residue calmodulin (CaM), a signaling protein that rearranges in the presence of target proteins and calcium.[1] To understand the chemical scale mechanism by which such conformational transitions take place, one would ideally like to obtain atomic resolution "movies" (i.e. experimentally-constrained molecular dynamics simulations) of these protein motions. To generate such movies, one needs to label the protein with chromophores at many positions and observe the movement of those labels, much as motion capture technology is used in making animated movies. An ideal label would be one that is "non-invasive," so that the chromophore does not alter the movements of the protein and can be placed at many locations to gather sufficient data to capture the protein motion.

Several methods exist for tracking protein dynamics, such as NMR, force microscopy, multidimesional IR, and fluorescence techniques using distance dependent chromophore interactions such as Förster resonance energy transfer (FRET).[2-5] Of these techniques, we find fluorescence most appealing because it is best suited to large proteins, it can be used to acquire real time data on nanosecond protein motions, it is relatively easy to carry out at the single molecule level, and it can be used in cells or complex mixtures.[6-10] These aspects are important because many of the most interesting and physiologically significant conformational changes inherently require larger proteins, because these transitions may involve several pathways over a broad potential energy surface, and because their mechanisms may be highly dependent on interactions with other proteins.

The most widely used method for fluorescently-tagging proteins employs the genetic fusion of a variant of the green fluorescent protein (GFP) from *A. victoria* to the protein of interest.[11, 12] GFP fusions are easy to prepare by standard cloning methods, but the large size of GFP (268 amino acids) limits its utility in observing the motions of proteins that are often of comparable size (e.g. CaM, Fig. 1).[13] Labeling proteins with small organic molecules like fluorescein, either during or after translation, introduces a much less structurally-perturbing probe.[14] However, many positions in the protein cannot accommodate these polycyclic organic chromophores. The bulk of GFP and fluorescein derivatives not only limits the number of places that these labels can be placed, but raises the concern that the label itself alters the observed motion. We believe that the thioamide – sulfur replacement of oxygen in the peptide backbone – provides a nearly optimal label: one that is extremely small and compatible with virtually any position in the protein.

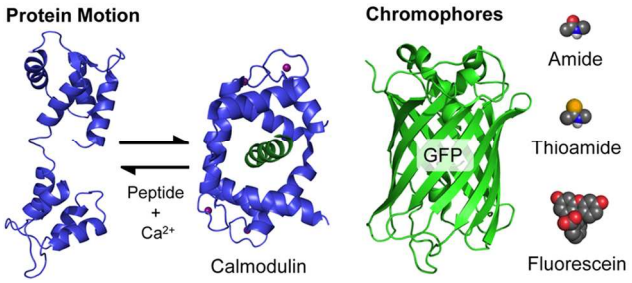

Fig. 1. Protein Chromophore Scale. Common biological chromophores are too large to be placed at many positions in a protein to monitor dynamics. Left: Conformational change in calmodulin upon binding Ca^{2+} and substrate peptide (PDB IDs 1CFD, 1SY9).[15, 16] Right: Common biological chromophores, GFP (1GFL)[17] and fluorescein, compared to an oxoamide and a thioamide. All molecules shown on the same scale.

Thioamides (denoted by a prime symbol, e.g. Leu′ or L′ and Ala′ or A′ in Fig. 2) are not emissive chromophores, but they can

quench fluorescence in a distance dependent manner and thus report on conformational changes in proteins. Placement of a thioamide at a position that does not move relative to the donor fluorophore will mean that the change in fluorescence is small regardless of the size of the conformational change (Fig. 2, Bottom). Placement at a site that moves relative to the fluorophore will register a large change in fluorescence (Fig. 2, Top). A thorough understanding of the distance dependence of fluorophore quenching by thioamides can be used to translate these changes in fluorescence into interchromophore distances. If analogs of the 20 natural amino acids can be made and incorporated at many sites in the protein, one should be able to gather enough time-dependent distance measurements to model the global conformational change.

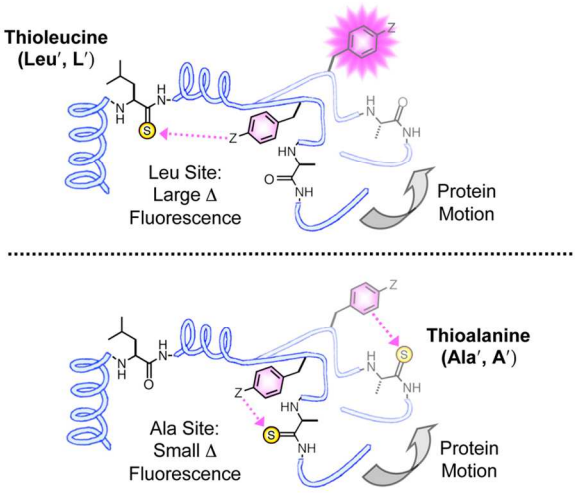

Fig. 2 Tracking Motion with Thioamide Quenching. Top: Placement of the thioamide in a region with large conformational changes gives a large change in fluorescence. Bottom: Placement at a position that does not move relative to the fluorophore gives a small change in fluorescence.

We have identified two types of fluorophore/thioamide interactions, FRET based quenching of UV fluorophores such as cyanophenylalanine (Cnf) and photoinduced electron transfer (PET) based quenching of visible wavelength fluorophores such as acridonylalanine (Acd) and fluorescein (Fam). These fluorophores can be used in distinct ways. FRET probes allow for rigorous distance determination, but cannot be used in the presence of Trp or Tyr. PET probes can be selectively excited in the presence of Trp, Tyr, and even cofactors such as Heme, because no spectral overlap with the thioamide is required. However, the distance dependence of PET quenching is less straightforward than FRET, so PET provides only rough proximity information.[18] We see these methods as complementary.

Trp and Tyr form a special category: these endogenous fluorophores are not particularly useful in monitoring distances, since many copies are usually present in the protein, but thioamide quenching of multiple Trp and Tyr residues can be used to determine binding constants and rates for protein/protein interactions. The donor fluorophores listed in Figure 3, along with thioamide analogs of the natural amino acids, constitute a chromophore toolbox for monitoring protein folding, interactions, and conformational changes.

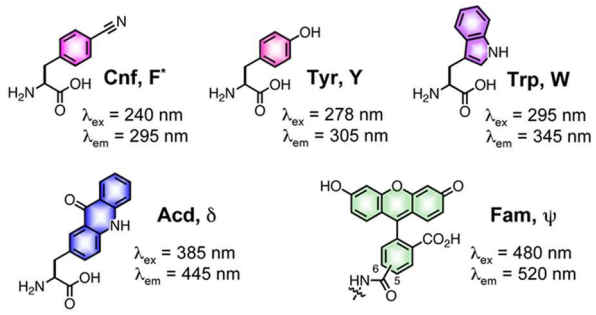

Fig. 3 Examples of Fluorophore Classes. Cyanophenylalamine (Cnf) and Tyr quenching have strong FRET components. Trp quenching is largely PET-based. Acridonylalanine (Acd) and fluorescein (Fam) quenching is entirely PET based. Fluorophore applications in thioamide quenching studies depend on size and excitation wavelength.

Thioamides are certainly not a stand alone solution to a problem as complex as protein conformational change. In fact, we also use "conventional" FRET approaches in our laboratory to track motions in signaling proteins like CaM as well as dynamic misfolding of amyloidogenic proteins such as α-synuclein (αS), which contributes to Parkinson's disease pathology.[19, 20] The development of thioamide quenchers provides a powerful new tool for any laboratory interested in protein dynamics – a small probe for short range measurements to complement longer range probes such as fluorescein/tetramethylrhodamine (working distance 25 to 75 Å).[21] This perspective includes four core sections designed to allow the user to determine how to best use thioamides as conformational probes. The sections are written so as to be readable in any order, according to the interest of the reader. For this reason, a list of all abbreviations used are collected at the end of the perspective for easy reference. Since the topics in this perspective could potentially encompass a large number of fluorophores, many proteins, and many techniques, we have limited our in-depth discussion to cases involving the fluorophores shown in Fig. 3. The concepts discussed are easily applied to other protein systems or chromophores.

2. The Impact of Thioamides on Protein Structure

A thorough understanding of the effect of thioamides on protein folding and structure can help to delineate the scope of our method and enable rational choices of probe location. Thioamides are nearly isosteric with the natural oxoamide found in the peptide backbone, but there are some subtle differences.

2.1 Physical properties of oxoamides and thioamides

The physical properties of oxoamides and thioamides are summarized in Table 1. Sulfur has a larger van der Waals radius than oxygen, and the thiocarbonyl bond is somewhat longer than the oxocarbonyl bond. The NH pK_a is substantially lower for the thioamide than the oxoamide. This can be rationalized by considering that the relative contribution of resonance structure B is greater for thioamides than for oxoamides.

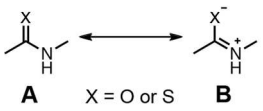

While this pK_a difference is unlikely to lead to deprotonation of the thioamide at a pH near 7, it reflects a more significant polarization of the NH bond that will impact hydrogen bonding. Thus, the thioamide NH is a stronger hydrogen bond donor than the oxoamide NH, while the sulfur is a slightly weaker hydrogen bond acceptor than the corresponding oxygen.[22, 23] Recently, Raines and coworkers have shown that thioamide interactions may have stabilizing effects via n-π* (from one thioamide unit to another carbonyl unit) interactions in certain turn geometries.[24] The barrier to rotation about the C–N bond is higher for thioamides, which may alter secondary structure despite the fact that most amides exist predominantly in the *cis* form and that interconversion is slow (s^{-1}) even for the lower barrier oxoamide.[25-28] Most backbone amide isomerizations in proteins require catalysis of some sort, but there may be noticable effects on uncatalyzed folding rates.

Table 1 Properties of amide bonds

	Oxoamide	Thioamide
van der Waals Radius (Å)[29]	1.40	1.85
C=X Bond Length (Å)[30]	1.23	1.71
C=X BDE[a] (kcal/mol)[31]	170	130
N-H pK_a[31]	17	12
C-N Rotational Barrier (kcal/mol)[27]	17	22
π–π* Absorption (nm)[32, 33]	200	270
E_{Ox} (V vs. SHE)[34]	3.29	1.21

[a] BDE = Bond Dissociation Energy.

The properties most relevant to our spectroscopic studies are the red shift in the carbonyl π-π* absorption and the lower oxidation potential of the thioamide. The change in the absorption maximum to ~ 270 nm allows the thioamide to have spectral overlap resulting in FRET interactions with Cnf and Tyr (see Fig. 5). The ~ 2 V change in oxidation potential allows the thioamide to be competitive in fluorophore PET quenching processes with other easily oxidized amino acids such as Trp or Cys. As described below, fluorophores which can be quenched by thioamides via PET can be easily identified through a calculation of ΔG_{ET} using the Rehm-Weller formalism.

2.2 Thioamide effects on protein folding

Several independent studies have examined the effect of thioamide substitution on the thermodynamic stability of α-helices and β-sheets. In α-helices, thioamide substitution at the C-terminus (within the last four residues) is expected to be tolerated, as the thiocarbonyl would not participate in hydrogen bonding at these sites. Other positions within the tightly packed helix were initially proposed to be unable to accommodate the increase in the (thio)amide-amide hydrogen bond distance or the larger size of the sulfur atom.[35] Miwa *et al.* prepared thioamide analogs of GCN4, a 35-residue helical peptide that dimerizes to form a parallel, two-stranded coiled-coil.[36] Circular dichroism (CD) measurements confirmed that thioamide substitution (at either the C-terminus or in the middle of the helix) yielded structures that were similar to those formed by the native peptide. The melting temperatures (T_ms) of the folded coiled-coils were derived by measuring the temperature-dependent change in the CD signal corresponding to helical content. A slight increase in T_m was observed for the peptide containing a thioamide near the center of the helix, suggesting that the increase in hydrogen bond strength conferred by the thioamide NH may enhance thermal stability in a position-dependent manner. In a separate study, Fischer, Kiefhaber, and coworkers introduced single thioamide substitutions at a central or an N-terminal position in an alanine-based helical peptide.[37] CD measurements revealed that incorporation of an Ala′ residue at either location led to helix destabilization similar in magnitude to that observed for a Gly substitution at each respective position (roughly 1.7 kcal/mol). (See Fig. 4, Left) It should be noted that this study differs significantly from the Miwa α-helix study in that the dimeric nature of GCN4 may also be influenced by thioamide incorporation, whereas the artificial α-helices in this study are monomeric and may provide a more direct assessment the impact of thioamides on the α-helix itself. Taken together, these results demonstrate that the effect of thioamide incorporation on α-helix stability may ultimately be dependent on the position in question.

To determine whether a thioamide linkage is compatible with β-sheet secondary structure, Miwa *et al*. prepared a thioamide-containing β-hairpin peptide, comprised of two antiparallel strands joined by a type II′ β-turn.[38] To minimize perturbation of the hairpin structure, the thioamide residue was inserted into the *i* + 2 position of the β-turn. In this position, the thiocarbonyl points toward the exterior of the hairpin, while the thioamide NH can still participate in an interstrand hydrogen bond. NMR and CD experiments confirmed that the hairpin conformation and stability were similar to that of the corresponding oxoamide peptide. (See Fig. 4, Middle) More recently, Gai, Degrado, and coworkers used thioamides to site-specifically examine the role of interstrand hydrogen bond formation in the folding of a stable monomeric β-hairpin known as tryptophan zipper (Trpzip).[39] In these studies, thioamide residues were placed in a manner such that the thiocarbonyl would be forced to participate in backbone-backbone hydrogen bonding throughout the β-hairpin sequence. Analysis of CD thermal melting curves for the mutant peptides revealed that the degree of β-hairpin destabilization depended on the position of the interstrand hydrogen bond being perturbed, with the effect far less pronounced at the terminal region of the hairpin. To further examine the mechanistic basis of thioamide-induced destabilization, the folding and unfolding rates of the mutant β-hairpins were determined by measuring their relaxation rates in response to a laser-induced T-jump using time-resolved IR spectroscopy. Thioamide incorporation at the turn region slowed down the rate of folding, whereas incorporation at the terminal region dramatically increased the rate of unfolding. Similar to observations in thioamide-containing α-helices, the effect of thioamide substitution into β-sheets is likely to be dependent on the position of incorporation and on whether the residue is involved in the formation of a key hydrogen bond in the native sequence.

Although thioamide substitution has been investigated in model peptides, there are few examples describing how thioamide incorporation into full-length proteins affects their ability to fold or function. To date, only one protein is known to naturally contain a thioamide linkage. Methyl-coenzyme M reductase, an enzyme that contains a thioglycine residue near its active site, catalyzes the final methane-forming step in methanogenic archaea.[40, 41] It has been proposed that the embedded thiocarbonyl moiety may work as a redox active one-

electron relay system to facilitate the oxidation and reduction of cofactor and substrate.[42] The X-ray crystal structure of Methyl-coenzyme M reductase has been determined, providing insight as to the geometry that thioamide residues adopt in complex folded proteins. (See Fig. 4, Right) The Gly′ residue is not located in a canonical α-helix or β-sheet. The thiocarbonyl length is extremely long (1.8 Å) and the C-N bond length is very short (1.3 Å), consistent with the predominance of resonance structure B as a representation of the thioamide. As one might expect, the hydrogen bond to sulfur is unusually long (3.5 Å) as compared to a typical backbone hydrogen bond in a protein (~ 3.0 Å). However, no increase in thioamide NH hydrogen bond donor strength is apparent, as the NH hydrogen bond is not unusually short (3.1 Å). Since Methyl-coenzyme M reductase has presumably evolved to take advantage of this specialized Gly′ residue, it is not clear that this information has general implications for the introduction of thioamides into existing secondary structures.

Fischer and coworkers have been able to demonstrate that a thioamide can be chemically installed into a different enzyme without perturbing its inherent activity.[43, 44] Ribonuclease (RNase) S, originally generated by cleaving RNase A into two fragments using subtilisin, is comprised of the separated S-peptide (residues 1 to 20) and the S-protein (residues 21 to 124). In solution, the S-protein is inactive but folded, whereas the S-peptide is disordered.[45] Upon binding to the S-protein, residues 3-13 of the S-peptide adopt an α-helical structure, yielding a catalytically active bimolecular complex. To monitor backbone hydrogen bond formation in the transition state of the S-peptide/S-protein association, single thioamide substitutions were introduced into different positions between residues 1 and 15 of the S-peptide. All of the S-peptide mutants bound to the S-protein to generate catalytically active complexes. However, isothermal titration calorimetry (ITC) experiments revealed that the thermodynamic stability of each mutant RNase S complex was reduced to varying extents, ranging from 0.6 to 4.7 kcal/mol. These results indicate that some thioamide substitutions can be tolerated in full-length proteins without grossly perturbing their native state or function.

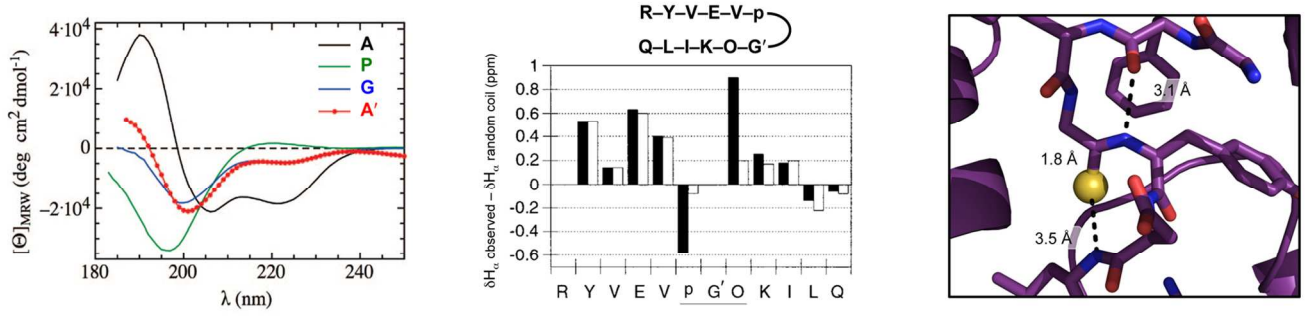

Fig. 4 The Impact of Thioamide Substitution on Protein Folding. Left: Circular dichroism (CD) analysis of α-helical peptide sequences by Reiner *et al*. showed that Ala′ substitution can be comparably destabilizing to glycine substitution.[37] Adapted figure reproduced with permission from the American Chemical Society. Middle: NMR analysis of a β-turn sequence by Miwa and coworkers showed that Gly′ was compatible with turn formation (p indicates D-proline).[38] Adapted figure reproduced with permission from the American Chemical Society. Right: The geometry of a hydrogen-bonded Gly′ residue can be seen in the sole structurally-characterized example of a full-length protein containing a thioamide residue, Methyl-coenzyme M reductase (PDB ID 1MRO).[41]

In general, one must carry out structural or functional analyses to determine whether a particular thioamide substitution is perturbative. Fortunately, there are a variety of structural and biophysical assays that can be applied to study the impact of thioamide substitution on protein folding. CD is the simplest and most general method. Temperature-dependent CD can be used to measure protein T_ms as well as the (temperature-independent) ΔH_{vH} and ΔS_{vH} of unfolding via van't Hoff analysis. Alternatively, differential scanning calorimetry (DSC), which involves determining changes in the partial molar heat capacity of the protein at constant pressure, can be used to derive the temperature-dependent ΔH and ΔS of unfolding. In order to extract meaningful data from these experiments, one must always include an oxoamide control peptide or protein in the analysis. ITC can be employed to determine the binding affinity of thiopeptides for protein targets and to compare the enthalpic and entropic components of binding to the equivalent oxopeptides. However, the most complete structural information would come from high resolution X-ray crystal structures or 2D NMR studies. Our laboratory employs a combination of these techniques to gain a thorough understanding of how thioamide residues might influence protein structure and function.

3. Fluorophore/Thioamide Photophysics

To our knowledge, the first observation of fluorophore quenching by thioamides was made by Wickz *et al*., where Trp quenching was observed in neat propylene gylcol.[46] In a second example, Równicka-Zubik *et al*. observed quenching of the intrinsic fluorescence of bovine serum albumin by thiouracil.[47] However, neither group carried out systematic studies after these observations. Our first investigation of thioamide quenching used Cnf, which has sufficient spectral overlap with thioamide absorption to be used in FRET experiments.[48] Since thioamides are not emissive chromophores, energy transfer is manifested in quenching of the donor fluorescence. Subsequent investigations of Tyr and Trp quenching revealed the possibility of PET quenching by thioamides.[49] Through detailed studies of Trp, Acd, Fam and other fluorophores, we have outlined a PET quenching mechanism wherein the fluorophore is reduced and the thioamide is oxidized.[50, 51]

3.1 Cnf as a FRET donor

FRET pairs are characterized by the Förster radius (R_0), the distance at which energy transfer is half-maximal.[5] This distance is determined by using Equation 1.

$$R_0^6 = \frac{(9000)\ln(10)\kappa^2\Phi J}{128\pi^5 n^4 N_A} \quad (1)$$

where κ^2 is an orientation factor for the interaction of the transition dipoles of the donor and accceptor chromophores, Φ is the quantum yield of the donor, J is the spectral overlap integral, defined from the donor emission spectrum, $f_D(\lambda)$, and acceptor absorption spectrum, $\varepsilon_A(\lambda)$, as

$$J = \int_0^\infty f_D(\lambda)\varepsilon_A(\lambda)\lambda^4 d\lambda \quad (2)$$

n is the refractive index, and N_A ia Avagadro's number. The absorption spectrum of Leu′Ala methyl ester, as well as the emission spectra of Cnf, Tyr, and Trp are shown in Figure 5.[48, 49]

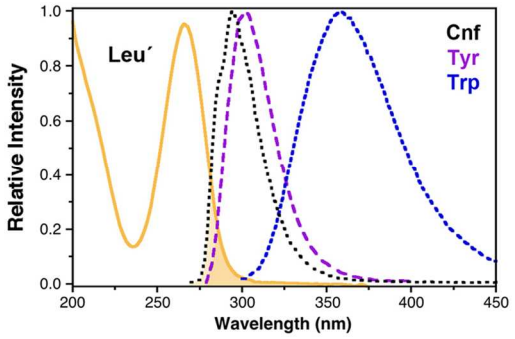

Fig. 5 Spectral Overlap of Thioamides with Cnf, Tyr, and Trp. Absorption spectrum of Leu′ thioamide (solid yellow line) and fluorescence emission spectra of Cnf, Tyr, and Trp (dashed black, purple, and blue lines, respectively). The shaded areas under the black and purple lines indicate the respective spectral overlaps of Leu´ with Cnf and Tyr.

Using these spectra to calculate J, and making the common assumption that the chromophores are randomly oriented so that $\kappa^2 = 2/3$, one obtains $R_0 = 15.6$ Å for the Cnf/thioamide pair. The distance dependence of the quenching efficiency (E_Q) is given by

$$E_Q(\text{FRET}) = \frac{1}{1+(R/R_0)^6} \quad (3)$$

where R is the distance between the two chomophores. Thus, this FRET pair can be used to measure distance changes in the 8 to 32 Å range. The distance dependence of this interaction was verified through the examination of a series of peptides in which rigid polyproline (Pro_n, n = 2 – 10) spacers were used to control the distance between Cnf and Leu′.[48] Quenching efficiency was determined as

$$E_Q = 1 - F_{Thio}/F_{Oxo} \quad (4)$$

where F_{Thio} is the fluorescence intensity of a given Leu′Pro_nCnf peptide, and F_{oxo} is the fluorescence of the oxoamide control peptide LeuPro_2Cnf. Interchromophore distances were determined from the average separations of the dipole midpoints in molecular dynamics (MD) simulations of the peptides in explicit water. A plot of the E_Q data for this series of peptides is shown in Figure 6.

As one can see, the experimental data match the prediction from Equation 3 (Fig. 6, solid lines) quite well. It should be noted that these data could also be fit to a Dexter mechanism, in which transfer occurs by oribital overlap, using Equation 5.[52]

$$E_Q(\text{Dexter}) = \frac{1}{1+\frac{2\pi}{\hbar}KJ_{Dex}e^{\left(-\frac{2R}{L_{Dex}}\right)}} \quad (5)$$

Here, the normalized spectral overlap inegral J_{Dex}, is given by

$$J_{Dex} = \int_0^\infty f_D(\lambda)\bar{\varepsilon}_A(\lambda)d\lambda \quad (6)$$

L_{Dex} is the sum of the chromophore raddii, K is a scaling factor, and again, R is the interchromophore distance. The fit to Equation 5 is shown as a dashed line in Figure 6. Although the Cnf proline ruler experiments could not clearly distinguish between these two mechanisms, subsequent experiments would allow us to do so (see Section 5.2).

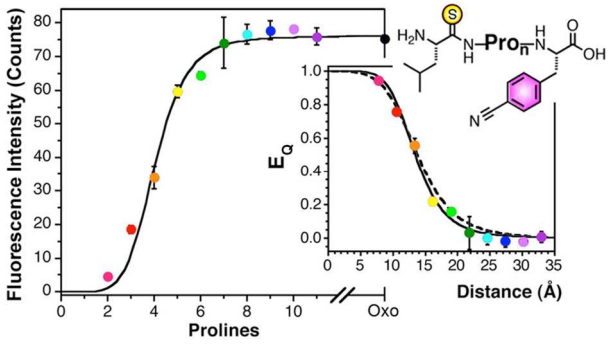

Fig. 6 Cnf/Thioamide Polyproline Ruler. Distance-dependence of Cnf-to-thioamide energy transfer from Förster theory (black line) compared to data from polyproline ruler experiment (colored points). Inset: E_Q fitted to the primary data (points colored as in intensity plot) according to Equations 1, 2, and 3 (solid line) or Equations 5 and 6 (dashed line), compared to interchromophore distances from MD simulations.

3.2 Tyr and Trp as FRET and PET donors

We have also carried out studies of the major intrinsic protein fluorophores, Trp and Tyr.[49] As one can see in Figure 5, the Tyr emission spectrum has moderate overlap with the thioamide absorbance spectrum, but the Trp emission spectrum has almost no overlap, yielding R_0 values of 13 Å for Tyr and 4 Å for Trp. We synthesized polyproline rulers for Tyr and Trp of the sort described for Cnf above. The E_Q values determined for these rulers are shown in Figure 7. There is a large disparity between the prediction from Förster theory and the observed E_Q profile for Tyr, and especially for Trp. In the case of Tyr, the difference may be due to a combination of FRET and Dexter processes. In the case of Trp, FRET is clearly not a significant factor, but a Dexter mechanism is possible. Although the Dexter mechanism requires spectral overlap, J_{Dex} does not impact the distance dependence in Equation 5. Fits of the Tyr and Trp E_Q data to Equation 5 are shown as dashed lines in Figure 7. We also considered the possibility of quenching through PET. A simple

distance-dependent quenching model for PET was fit to the Trp and Tyr polyproline ruler data.[53, 54]

$$E_Q(\mathrm{PET}) = \frac{1}{1 + k_a e^{\left(\frac{2R-a}{r_e}\right)}} \quad (7)$$

In Equation 7, a is the distance of closest approach of the chromophores, r_e is the so-called characteristic distance, and k_a is the rate of the reaction at the distance a. As before, R is defined as the distance between the chromophores. Both the Dexter and PET models fit the data equally well, which is expected, since they have the same exponential form.

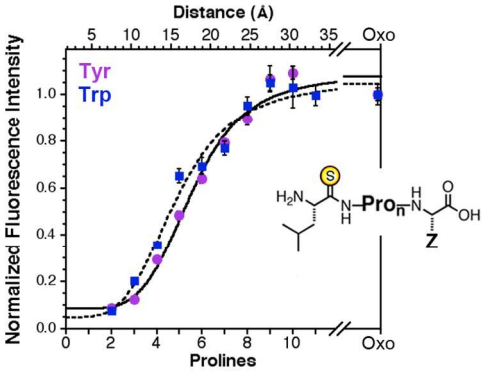

Fig. 7 Tyr/Thioamide and Trp/Thioamide Polyproline Rulers. The fluorescence emission at 305 nm of Leu′-Pro$_n$-Tyr (purple circles) or emission at 355 nm of Leu'-Pro$_n$-Trp (blue squares). The "Oxo" data point indicates the fluorescence of Leu-Pro$_2$-Tyr or Leu-Pro$_2$-Trp. Fits of the data to Equation 7 are shown for both Tyr (solid line) and Trp (dashed line). Distances were determined from MD simulations.

To further explore Trp and Tyr quenching, we carried out studies of thiopeptide binding to CaM.[49] CaM was an ideal test case, because it binds short helical peptides in a well-defined, high-affinity (nM K_D) cleft, and it has only two native Tyr and no Trp, so it was easy to generate mutants in which a single Trp or Tyr at positon 100 or 139 served as the donor fluorophore.[55, 56] In all cases, an N-terminally Phe′-labeled peptide (pOCNC, derived from a cyclic nucleotide-gated channel)[57] was mixed with the CaM mutant in question and the fluorescence of the bound complex was monitored. Quenching by pOCNC-F′$_1$ reported qualitatively on chromophore separation (position 100, 20 Å away, was quenched less; position 139, 15 Å away, was quenched more),[15] but there was no quantitative agreement with predictions from Förster theory for either Tyr or Trp donors. Of course, for Trp, no quenching via FRET was expected because of the lack of spectral overlap.

The Trp mutant experiments demonstrated that thioamide PET quenching of Trp was a viable way of probing interactions in folded proteins, and led to our further exploration of PET interactions. The poor agreement of the Tyr quenching data with FRET models in both the polyproline ruler and CaM experiments led us to question the use of Tyr as a donor in any distance measurement experiments. In general, we have chosen to use Cnf rather than Tyr in most FRET applications. In addition to excellent agreement of Cnf quenching with the expected E_Q values in several model systems (see sections 3.1, 5.1, and 5.2), Cnf has significant advantages over Tyr as a chromophore. The extinction coefficient of Cnf at its excitation wavelength (ε_{232} = 13,330 $M^{-1}cm^{-1}$)[58] is much higher than that of Tyr (ε_{278} = 1280 $M^{-1}cm^{-1}$), and thioamides absorb stongly at the excitation wavelength of Tyr (ε_{278} = 10,240 $M^{-1}cm^{-1}$), which may compromise its utility as a donor fluorophore. The only real advantage of Tyr over Cnf, its genetic encodability, has been negated by incorporation of Cnf through the Schultz unnatural amino acid mutagenesis method. (See section 4.3)

3.3 Red-shifted PET donors

Following on our observation that Trp can be quenched by thioamides, we explored thioamide PET by determining the levels of quenching for a large number of red-shifted fluorophores including acridone, 7-azatryptophan, carboxyfluoresecin, and boron-dipyrromethene (BODPIY).[50, 51] The emission spectra of these chromophores have no spectral overlap with thioamide absorption, therefore we could test them by simply performing Stern-Volmer quenching studies. The dyes were each mixed with 50 mM acetamide or thioacetamide and then the steady state fluorescence was measured to determine a quenching efficiency (E_Q^{SS} in Table 2) according to Equation 4. We also carried out time-correlated single photon counting (TCSPC) experiments to determine the fluorescence lifetime (τ) of each fluorophore in the oxoamide and thioamide solutions. For these, we also computed quenching efficiency from the average lifetimes (E_Q^{τ} in Table 2) according to Equation 4. We found that fluorophores across the visible emission spectrum could be quenched by thioamides.

The observed quenching can be rationalized through calculations of the free energy of electron transfer ($\Delta G°_{ET}$) using Equation 8.

$$\Delta G°_{ET} = F\{E°_{Ox}(\mathrm{D}) - E°_{Red}(\mathrm{A})\} - E_{0,0} + C \quad (8)$$

where F is the Faraday constant; E_{ox}(D) and E_{red}(A) are the oxidation and reduction potentials of the electron donor and acceptor molecules, respectively; $E_{0,0}$ is the zero vibrational electronic excitation energy of the fluorophore, calculated as the average energy of the absorption and emission wavelengths of the fluorescent transition; and C is a term accounting for Coulombic interactions, which is typically assumed to be negligible in water.

Table 2 Quenching of Red-Shifted Fluorophores[a]

Fluorophore (λ_{ex}, λ_{em})	E_Q^{SS} (%)	E_Q^{τ}	$\Delta G°_{ET}$ (eV)
Acridone (386, 446)	68 ± 1	67 ± 1	-0.13
NBD (467, 538)	27 ± 1	19 ± 1	-0.56
Carboxyfluorescein (488, 520)	44 ± 1	40 ± 1	-0.71
BODIPY FL (502, 510)	61 ± 4	55 ± 1	-0.39
Rhodamine R6G (526, 556)	16 ± 1	20 ± 1	-0.36
Texas Red (582, 602)	0	0	+0.01

[a] E_Q^{SS}, E_Q^{τ}, and calculations of $\Delta G°_{ET}$ found in Goldberg *et al.*[50, 51]

The values of $\Delta G°_{ET}$ in Table 2 were determined by assuming that the thioamide is the oxidized donor (D) and that the fluorophore is the reduced acceptor (A), using the thioamide oxidation potential in Table 1 and literature values (in most cases) for the fluorophore reduction potentials. It is possible that some fluorophores will be quenched through a different PET

mechanism, in which the thioamide is reduced. Quenching is depicted graphically in Figure 8.

Since the distance dependence of PET quenching is difficult to predict *de novo*, we have examined a number of model systems, with a particular focus on the fluorophores acridone and fluorescein. We have used acridone as the amino acid derivative acridon-2-ylalanine (Acd) and fluorescein as 5-carboxy (Fam) derivatives attached through either amide, maleimide-Cys, or triazole "click" linkages. We have found that quenching of Acd is possible in cases where the average separation of the chromophores is 10-15 Å (based on MD simulations), but that Fam quenching requires average separations near van der Waals contact with the thioamide for quenching. For example, in peptides where the fluorophore is separated from the thioamide by either polyproline or polyglycine linkers, Acd quenching occurs in Pro_2 and Pro_3 peptides. On the other hand, no Fam quenching is observed in polyproline peptides, but quenching is observed when the thioamide is separated by glycine linkers longer than Gly_2. We believe that this is because van der Waals contact with the thioamide is not permitted by the short Gly_2 linker and the rigid polyproline linkers. The longer excited state lifetime of Acd gives it more time to be quenched, wherease Fam is only quenched if the thioamide is close enough to transfer an electron before emission occurs. The differences in photophysical properties mean that Acd and Fam have different effecive quenching radii, so that when quenching is observed, we infer that Acd is within 10-15 Å of the thioamide whereas Fam must be at van der Waals contact.

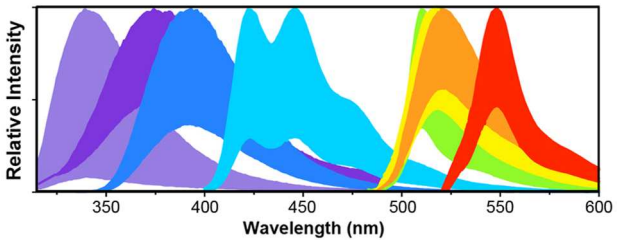

Fig. 8 PET-based Fluorophore Quenching by Thioamides. Fluorescence emission of (from left) 5-hydroxytryptophan, 7-azatryptophan, 7-methoxycoumarin, acridone, 5-carboxyfluorescein, Alexa Fluor 488, BODIPY FL, and Rhodamine 6G in the absence (shaded spectrum) or the presence of a thioamide (open spectrum below).

4. Synthesis of Thioamide Labeled Proteins

The primary focus of this perspective is on the photochemistry of these systems, however, we include a brief description of their incorporation into peptides by solid phase peptide synthesis (SPPS) and the ligation of these peptides to expressed proteins to form full-sized proteins.

4.1 Chemical synthesis of thiopeptides

Thioamide-containing peptides of up to forty amino acids can be routinely synthesized on solid phase using Fmoc chemistry. Thioamides are incorporated from benzotriazole precursors which can be synthesized from the corresponding Fmoc-protected amino acid in three steps.[38, 59, 60] Successful thioamide incorporation from benzotriazole precursors has been reported for the aliphatic amino acids Ala, Phe, Ile, Leu, and Val using Boc-protected diaminobenzene or for Asp, Glu, Ser, Thr, and Lys using *p*-deactivated diaminobenzene (Fig. 9). Conceivably, a thioamide analog of any of the natural amino acids can be incorporated into proteins using appropriate protecting group manipulations.

4.2 Preparation of full-sized thioproteins by ligation

To insert thioamides into full-sized proteins, one can make use of native chemical ligation (NCL) reactions.[61] NCL is a valuable method for synthesizing proteins by fragment condensation of a C-terminal thioester peptide and an N-terminal Cys peptide in buffered aqueous media. In our initial investigations of NCL reactions between short peptides, we found that thioamides can be placed at nearly any position in the thioester or Cys peptide fragments. Furthermore, we have found that thioamides could be used in NCL reactions in which the N-terminal Cys fragment was expressed as a protein construct in *E. coli* (expressed protein ligations). The C-terminal thioseter can also be generated from an expressed protein by making use of an intein fusion. Since some proteins, such as αS and CaM, lack any endogenous Cys, we have also made use of methods developed in our laboratory to attach Cys analogs such as homocysteine (as Hcm, protected with a thiomethyl group) to expressed proteins to enable "traceless" ligations.[62] In general, we minimize the need for manual SPPS by maximizing the role of biosynthesis in preparing labeled proteins. These ligations can limit the portion that must be prepared by SPPS to a few amino acids around the thioamide. SPPS is deemed necessary for the incorporation of backbone thioamide modifications, but sidechain fluorophores like Cnf can be incorporated during ribosomal biosynthesis.

4.3 Fluorophore incorporation by unnatural mutagenesis

To track folding events by intramolecular FRET or PET, we must not only incorporate thioamides into full-length proteins, but donor fluorophores as well. Although these could be incorporated into proteins *via* NCL, because we are not modifying the backbone we can simplify the SPPS steps and increase protein yields using the unnatural amino acid (Uaa) mutagenesis techniques developed by Schultz.[63] Briefly, Uaa mutagenesis is accomplished by transforming *E. coli* with two plasmids, one coding for an unnatural amino acid tRNA synthetase (UaaRS) with $tRNA_{CUA}$ (recognizing a UAG stop codon) and one coding for the protein of interest with a TAG codon insert. The cells are then grown with the unnatural amino acid (e.g. Cnf), and the expressed protein is purified for fluorescence studies.

4.4 Double-labeling by unnatural mutagenesis and ligation

Recently, we have shown that one can combine unnatural mutagenesis with NCL to install thioamide probe pairs into full-length proteins for folding studies.[64] To synthesize double-labeled constructs containing a thioamide at the N-terminus, we can express a Uaa-containing C-terminal protein fragment that also contains an N-terminal Cys for ligation. This fragment can then undergo NCL with a thioamide-containing thioester peptide to yield the full-length double-labeled protein. Alternatively, we can use intein technology to generate a Uaa-containing N-terminal protein fragment with a C-terminal thioester linkage. The expressed fragment can then be condensed with a C-terminal thioamide-labeled peptide bearing the requisite N-terminal Cys

for ligation. While these methods allow us to produce a variety of double-labeled proteins, they require the presence of Cys at the ligation site. We have recently combined Uaa mutagenesis with ligation at Hcm to synthesize double-labeled proteins in a traceless and efficient manner.[65]

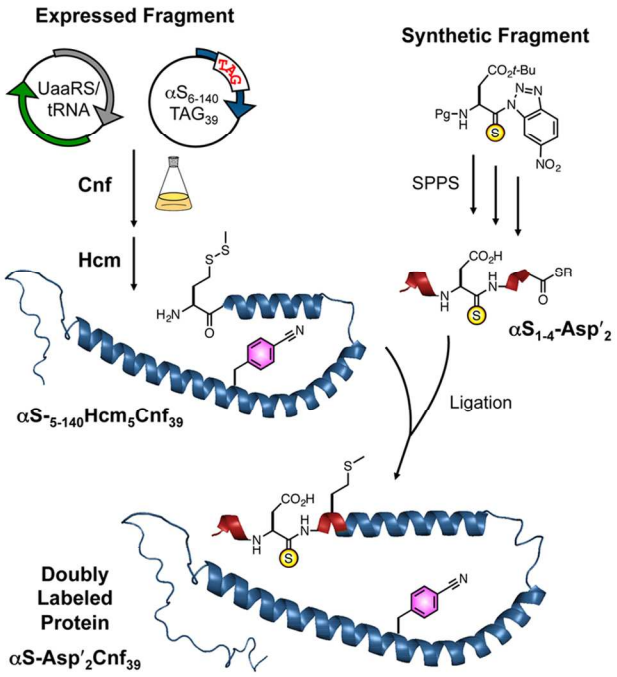

Fig. 9 Synthesis of Fluorophore/Thioamide Labeled Proteins by a Combination of Unnatural Mutagenesis and Native Chemical Ligation. A protein fragment containing a fluorescent unnatural amino acid (e.g. Cnf) can be expressed in *E. coli* grown in specialized media after transformation with plasmids encoding a UaaRS and $tRNA_{CUA}$. The fragment is then purified for ligation to a synthetic peptide containing a thioamide. For Cys-free ligations, homocysteine (as Hcm) can be appended to the expressed fragment using a transferase enzyme.

5. Benchmarking Studies in Model Systems

In order to verify that our thioamide quenching probes can provide useful information on conformational changes, we have performed proof-of-principle folding and proteolysis experiments using well-characterized model protein systems.

5.1 Villin headpiece with Cnf and Acd

HP35, a variant of the villin headpiece subdomain, is known to adopt a compact helical structure in which the N- and C-termini are in close proximity (within 20 Å).[66] Since global unfolding of HP35 leads to a significant increase in the distance between the termini, we chose to incorporate Leu′ at the N-terminus and Cnf at the C-terminus for FRET experiments.[48] Additionally, because Cnf is excited at 240 nm and fluoresces with a maximum at 295 nm, we also mutated Trp_{23} to Phe to ensure that Trp fluorescence (arising from direct excitation or from Cnf/Trp FRET) would not convolute the spectral data. By obtaining temperature-dependent CD measurements, we were able to show that the T_m of the double-labeled HP35 variant (HP35-$L'_1F_{23}F^*_{35}$) was similar to that of the corresponding oxoamide control protein (HP35-$F_{23}F^*_{35}$), indicating that the thioamide replacement did not exert a measureable effect on overall stability. We were then able to demonstrate that the thermal denaturation of HP35 can be accurately monitored by observation of Cnf/thioamide FRET. Quenching efficiency (E_Q) was determined over a range of temperatures (5 to 75 ºC) by comparing the fluorescence intensity of the thioamide protein to the oxoamide control. Upon converting E_Q to distance using Förster theory, we determined that the separation between the termini of HP35 increased from 21 Å in the folded form to a distance beyond that measurable by our probe pair (32 Å) in the unfolded state.

Having demonstrated that we can use thioamide/Cnf FRET to monitor unfolding of HP35, we wished to determine whether a thioamide/Acd PET interaction could also be used to track this conformational change.[51] We synthesized a similarly double-labeled HP35 variant for PET studies bearing Leu′ at the N-terminus and Acd at the C-terminus (HP35-$L'_1\delta_{35}$). Since Acd absorbance is significantly red-shifted from tryptophan, mutation of Trp_{23} to Phe was no longer necessary. Temperature-dependent CD measurements indicated that the T_m of HP35-$L'_1\delta_{35}$ was comparable to its corresponding oxoamide control peptide (HP35-δ_{35}). Steady-state fluorescence measurements of the proteins showed that Acd in HP35-$L'_1\delta_{35}$ was quenched 16% relative to HP35-δ_{35} at 1 ºC. During thermal unfolding of HP35-$L'_1\delta_{35}$, we observed an initial increase in E_Q that reached a maximum of 22% at 66 ºC. Since thioamide PET quenching of Acd is dependent on chromophore contact, we believe that this initial rise in E_Q is the result of enhanced flexibility of the termini leading to more productive intramolecular collisions. Upon increasing the temperature further, E_Q rapidly decreased to 15%. By comparing this observed change in E_Q as a function of fraction folded to the distance constraints we previously measured by thoiamide/Cnf FRET, we can attribute the decline in PET quenching to an increase in separation between the N- and C- termini at higher temperatures.

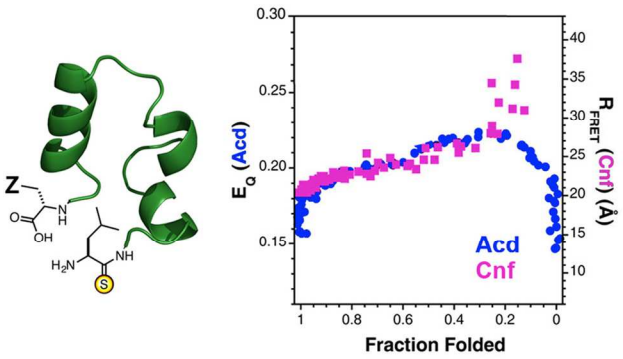

Fig. 10 Villin Headpiece HP35 Experiments. Left: Structure of HP35-Leu'$_1$Acd$_{35}$ modified from PDB 1VII.[67] Right: Steady-state quenching efficiency (E_Q(Acd); blue circles) as a function of fraction of protein folded determined by CD spectroscopy and the separation of the N- and C-termini as a function of fraction folded determined by a FRET experiment with thioamide quenching of Cnf (R_{FRET}(CNF); magenta squares). Adapted figure reproduced with permission from the American Chemical Society.[51]

5.2 Calmodulin with Cnf

To characterize intermolecular thioamide quenching of Cnf in full-sized proteins, we examined ligand binding to the protein CaM in a similar manner to the experiments performed with Tyr and Trp described in section 3.2.[64] Since Cnf cannot be

selectively excited in the presence of tyrosine, we mutated the native Tyr residues in CaM to Phe (CaM^F), allowing us to readily interpret our fluorescence data. Cnf can be site-specifically installed into full-length CaM using unnatural amino acid mutagenesis (see section 4.3). To test the full working-range of our probe pair, we used the existing NMR structure of the CaM/pOCNC complex[15] to design a library of pOCNC thiopeptides and Cnf-containing CaM mutants that allowed us to examine interchromophore distances spanning 8 to 31 Å. Three positions (F_{13}, F_{93}, and Y_{100}) were chosen for incorporation of Cnf. Three thiopeptide ligands were synthesized (pOCNC-F'_1, pOCNC-L'_{11}, and pOCNC-F'_{16}) in addition to an oxopeptide control (pOCNC). Native polyacrylamide gel electrophoresis (PAGE) analysis was performed to confirm that each CaM^F/pOCNC combination formed stable complexes in a 1:1 ratio. Upon addition of thiopeptide, we observed a decrease in Cnf emission relative to the corresponding oxopeptide complex. In order to accurately determine interchromophore distances based on our measured E_Q values, we first needed to determine the quantum yield of Cnf (which varied based on position of incorporation) in each CaM^FF*/pOCNC complex. By comparing the fluorescence emission of Cnf in each protein/ligand system to an equimolar solution of Cnf (as the free amino acid) we were able to correct for any environmental effects on Cnf quantum yield in the full-length proteins. The table in Figure 11 shows a comparison of the interresidue distances measured in our FRET experiments (R_{FRET}) to the corresponding distances from the NMR-derived CaM/pOCNC structure (R_{NMR}). Importantly, the dependence of E_Q on Cnf Φ supports a FRET-based quenching mechanism, as opposed to Dexter or PET mechanisms, for which the distance dependence is not altered by changes in donor Φ.

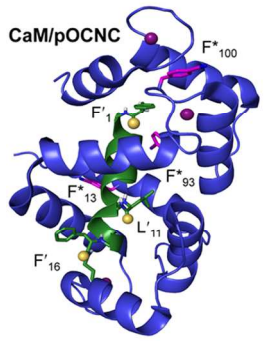

CaM/pOCNC Mutants (Φ)	% E_Q Obsvd	R (Å) FRET	R (Å) NMR
F^*_{13}/F'_1 (0.003)	11	13	14
F^*_{13}/L'_{11} (0.003)	37	11	14
F^*_{93}/F'_1 (0.014)	79	12	9
F^*_{93}/L'_{11} (0.014)	43	13	12
F^*_{100}/F'_1 (0.110)	25	20	19
F^*_{100}/L'_{11} (0.110)	17	21	24
F^*_{100}/F'_{16} (0.110)	10	23	31

Fig. 11 Calmodulin/Peptide Complex Experiments. Left: Cnf (pink) shown at three positions in CaM (blue protein) with three possible thioamide (yellow sphere) locations within pOCNC (green peptide). Ca^{2+} ions are shown as purple spheres. Adapted from PDB ID 1SYD using PyMol.[15] Right: Parameters used in comparison of CaM/pOCNC FRET and NMR data. Φ determined by comparison to fluorescence emission of 10 μM Cnf, Φ = 0.110. E_Q determined for 1:1 CaM/pOCNC complex. R_{FRET} calculated from E_Q using Equation 3. R_{NMR} is an average value calculated from the twenty lowest energy structures in PDB ID 1SYD.

Most of the experimentally obtained distance constraints are within 3 Å of the values observed in the NMR structure. These results clearly demonstrate that we can use thioamide/Cnf FRET to obtain structural information on protein complexes in a facile and accurate manner.

5.3 Profluorescent protease substrates

We have also demonstrated that fluorophore/thioamide pairs can be used to design profluorescent substrates for monitoring protease activity in real time. Since these tools will be most useful if the signal can be monitored in complex mixtures of other proteins, we use donors such as coumarin or fluorescein that are quenched via PET. The strategy, which is illustrated in Figure 12, employs a short peptide that is labeled with a thioamide and fluorophore on either side of a canonical protease sequence such that fluorescence is quenched. When the intervening amino acid sequence is cleaved by a proteolytic enzyme, the fluorophore and thioamide diffuse away from each other, leading to an increase in fluorescence. For example, cleavage of the substrate A'AFKGψ (ψ represents Fam-Cys) by trypsin is shown in Figure 12. Upon addition of trypsin to the peptide, we observed an increase in fluorescence at a rate consistent with previous measurements of trypsin kinetics using small peptide substrates. Control experiments with the corresponding oxoamide peptide (AAFKGψ) showed that the changes observed with A'AFKGψ could be exclusively attributed to thioalanine quenching of Fam.

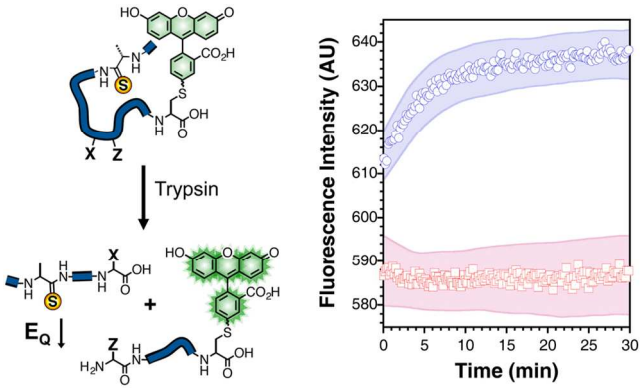

Fig. 12 Monitoring Protease Activity. Left: A cartoon illustrating the cleavage of a profluorescent peptide substrate by a protease. Right: Fluorescence of A'AFKGψ peptide in the presence (blue circles) and absence (red squares) of trypsin. Figure reproduced with permission from the American Chemical Society.[50]

We have evaluated thiopeptide substrates for a large number of proteases, including serine-, cysteine-, carboxyl-, and metallo-proteases, including trypsin, chymotrypsin, pepsin, thermolysin, papain, and calpain.[68] Importantly, we have found that thioamides are not perturbing to proteolysis rates when placed at locations a few amino acids removed from the scissile bond. We have demonstrated the value of our method in three model applications: 1) characterization of papain enzyme kinetics using rapid-mixing experiments, 2) selective monitoring of cleavage at a single site in a peptide with multiple proteolytic sites, and 3) analysis of the specificity of an inhibitor of calpain in cell lysates.

6. Conclusions

Over the previous four years, we have developed the thioamide as a versatile fluorescence quenching probe that is minimally-perturbing so that it can be placed at many locations in a protein sequence. While there are certainly technical challeneges yet to be overcome, we have shown that one can conceivably label any protein through semi-synthesis, provided that it can be

appropriately refolded. Thioamides can be paired with a variety of fluorophores to probe protein/protein interactions, protein folding or misfolding, and proteolysis. In our own laboratory, we have begun to apply thioamide probes to obtain dynamic structural information on the misfolding of αS in order to better understand its role in Parkinson's disease pathology. Since thiopeptide synthesis can be performed with minor modifications of standard peptide synthesis procedures, these methods should broadly accessible to the biochemistry and biophysics communities. In the coming years, we will further push the boundaries of thioamide applications, including their use in single molecule fluorescence experiments, their use in microscopy experiments in living cells, and their direct incorporation into proteins during ribosomal biosynthesis.

Abbreviations

Thioamide residues are represented by the one or three letter code of the equivalent oxoamide amino acids with a prime symbol (e.g. L′ or Leu′ represent thioleucine); Acd or δ, acridon-2-ylalanine; BODIPY, boron-dipyrromethene; CaM, calmodulin; Cnf or F*, *p*-cyanophenylalanine; Fam or ψ; carboxyfluorescein derivatives; FRET, Förster resonance energy transfer; NCL, native chemical ligation; PET, photoinduced electron transfer; SPPS, solid phase peptide synthesis; αS, α-synuclein; TCSPC, time correlated single photon counting; Uaa, unnatural amino acid; UaaRS, unnatural amino acid tRNA synthetase.

Notes and references

Department of Chemistry, University of Pennsylvania, 231 South 34th Street, Philadelphia, Pennsylvania 19104-6323 USA. Fax: +1-215-573-2112; Tel: +1-215-746-2221; E-mail:ejpetersson@sas.upenn.edu

† Electronic Supplementary Information (ESI) available: [details of any supplementary information available should be included here]. See DOI: 10.1039/b000000x/

‡ Footnotes should appear here. These might include comments relevant to but not central to the matter under discussion, limited experimental and spectral data, and crystallographic data.

1. S. W. Vetter and E. Leclerc, *Eur. J. Biochem.*, 2003, **270**, 404-414.
2. A. Borgia, P. M. Williams and J. Clarke, in *Ann. Rev. Biochem.*, 2008, vol. 77, pp. 101-125.
3. I. R. Kleckner and M. P. Foster, *Biochim. Biophys. Acta*, 2011, **1814**, 942-968.
4. A. Remorino and R. M. Hochstrasser, *Acc. Chem. Res.*, 2012, **45**, 1896-1905.
5. T. Forster, *Discuss. Faraday Soc.*, 1959, **No. 27**, 7-17.
6. M. P. Brown and C. Royer, *Curr. Opin. Biotechnol.*, 1997, **8**, 45-49.
7. M. R. Eftink, *Fluorescence Spectroscopy*, 1997, **278**, 221-257.
8. M. R. Eftink and M. C. R. Shastry, *Fluorescence Spectroscopy*, 1997, **278**, 258-286.
9. B. N. G. Giepmans, S. R. Adams, M. H. Ellisman and R. Y. Tsien, *Science*, 2006, **312**, 217-224.
10. B. Schuler and H. Hofmann, *Curr. Opin. Struct. Biol.*, 2013, **23**, 36-47.
11. M. Chalfie, Y. Tu, G. Euskirchen, W. W. Ward and D. C. Prasher, *Science*, 1994, **263**, 802-805.
12. R. Y. Tsien, *Ann. Rev. Biochem.*, 1998, **67**, 509-544.
13. D. W. Piston and G. J. Kremers, *Trends Biochem.Sci.*, 2007, **32**, 407-414.
14. A. R. Katritzky and T. Narindoshvili, *Org. Biomol. Chem.*, 2009, **7**, 627-634.
15. G. M. Contessa, M. Orsale, S. Melino, V. Torre, M. Paci, A. Desideri and D. O. Cicero, *J. Biomol. NMR*, 2005, **31**, 185-199.
16. H. Kuboniwa, N. Tjandra, S. Grzesiek, H. Ren, C. B. Klee and A. Bax, *Nat. Struct. Biol.*, 1995, **2**, 768-776.
17. F. Yang, L. G. Moss and G. N. Phillips, *Nat. Biotechnol.*, 1996, **14**, 1246-1251.
18. S. Doose, H. Neuweiler and M. Sauer, *ChemPhysChem*, 2009, **10**, 1389-1398.
19. P. K. Auluck, G. Caraveo and S. Lindquist, *Annu. Rev. Cell Dev. Biol.*, 2010, **26**, 211-233.
20. M. Drescher, M. Huber and V. Subramaniam, *ChemBioChem*, 2012, **13**, 761-768.
21. P. Wu and L. Brand, *Anal. Biochem.*, 1994, **218**, 1-13.
22. E. P. Dudek and G. Dudek, *J. Org. Chem.*, 1967, **32**, 823-&.
23. M. Hollosi, Z. Majer, M. Zewdu, F. Ruff, M. Kajtar and K. E. Kover, *Tetrahedron*, 1988, **44**, 195-202.
24. R. W. Newberry, B. VanVeller, I. A. Guzei and R. T. Raines, *J. Am. Chem. Soc.*, 2013, **135**, 7843-7846.
25. V. N. Balaji, S. Profeta and S. W. Dietrich, *Biochem. Biophys. Res. Commun.*, 1987, **145**, 834-841.
26. T. F. M. Lacour, H. A. S. Hansen, K. Clausen and S. O. Lawesson, *Int. J. Peptide Protein Res.*, 1983, **22**, 509-512.
27. K. B. Wiberg and D. J. Rush, *J. Am. Chem. Soc.*, 2001, **123**, 2038-2046.
28. K. B. Wiberg and D. J. Rush, *J. Org. Chem.*, 2002, **67**, 826-830.
29. A. Bondi, *J. Phys. Chem.*, 1964, **68**, 441-451.
30. M. R. Truter, *J. Chem. Soc.*, 1960, 997-1007.
31. T. Sifferlen, M. Rueping, K. Gademann, B. Jaun and D. Seebach, *Helv. Chim. Acta*, 1999, **82**, 2067-2093.
32. H. Basch, M. B. Robin and N. A. Kuebler, *J. Chem. Phys.*, 1967, **47**, 1201-&.
33. H. Hosoya, J. Tanaka and S. Nagakura, *Bull. Chem. Soc. Japan*, 1960, **33**, 850-860.
34. F. G. Bordwell, D. J. Algrim and J. A. Harrelson, *J. Am. Chem. Soc.*, 1988, **110**, 5903-5904.
35. T. F. M. Lacour, *Int. J. Peptide Protein Res.*, 1987, **30**, 564-571.
36. J. H. Miwa, L. Pallivathucal, S. Gowda and K. E. Lee, *Org. Lett.*, 2002, **4**, 4655-4657.
37. A. Reiner, D. Wildemann, G. Fischer and T. Kiefhaber, *J. Am. Chem. Soc.*, 2008, **130**, 8079-8084.
38. J. H. Miwa, A. K. Patel, N. Vivatrat, S. M. Popek and A. M. Meyer, *Org. Lett.*, 2001, **3**, 3373-3375.
39. R. M. Culik, H. Jo, W. F. DeGrado and F. Gai, *J. Am. Chem. Soc.*, 2012, **134**, 8026-8029.
40. S. Shima, M. Krueger, T. Weinert, U. Demmer, J. Kahnt, R. K. Thauer and U. Ermler, *Nature*, 2012, **481**, 98-101.
41. U. Ermler, W. Grabarse, S. Shima, M. Goubeaud and R. K. Thauer, *Science*, 1997, **278**, 1457-1462.
42. J. Kahnt, B. Buchenau, F. Mahlert, M. Kruger, S. Shima and R. K. Thauer, *FEBS J.*, 2007, **274**, 4913-4921.
43. A. Bachmann, D. Wildemann, F. Praetorius, G. Fischer and T. Kiefhaber, *Proc. Natl. Acad. Sci. USA*, 2011, **108**, 3952-3957.

44. D. Wildemann, C. Schiene-Fischer, T. Aumueller, A. Bachmann, T. Kiefhaber, C. Luecke and G. Fischer, *J. Am. Chem. Soc.*, 2007, **129**, 4910-4918.
45. R. T. Raines, *Chem. Rev.*, 1998, **98**, 1045-1065.
46. W. Wiczk, I. Gryczynski, H. Szmacinski, M. L. Johnson, M. Kruszynski and J. Zboinska, *Biophys. Chem.*, 1988, **32**, 43-49.
47. J. Rownicka-Zubik, A. Sulkowska, B. Bojko, M. Maciazek-Jurczyk, J. Pozycka, D. Pentak and W. W. Sulkowski, *J. Photochem. Photobiol. B*, 2009, **97**, 54-59.
48. J. M. Goldberg, S. Batjargal and E. J. Petersson, *J. Am. Chem. Soc.*, 2010, **132**, 14718-14720.
49. J. M. Goldberg, R. F. Wissner, A. M. Klein and E. J. Petersson, *Chem. Commun.*, 2012, **48**, 1550-1552.
50. J. M. Goldberg, S. Batjargal, B. S. Chen and E. J. Petersson, *J. Am. Chem. Soc.*, 2013, **135**, 18651–18658.
51. J. M. Goldberg, L. C. Speight, M. W. Fegley and E. J. Petersson, *J. Am. Chem. Soc.*, 2012, **134**, 6088-6091.
52. D. L. Dexter, *J. Chem. Phys.*, 1953, **21**, 836-850.
53. J. R. Lakowicz, *Principles of fluorescence spectroscopy*, Springer, 2006.
54. B. Zelent, J. Kusba, I. Gryczynski, M. L. Johnson and J. R. Lakowicz, *J. Phys. Chem.*, 1996, **100**, 18592-18602.
55. A. Crivici and M. Ikura, *Ann. Rev. Biophys. Biomol. Stuct.*, 1995, **24**, 85-116.
56. J. Haiech and M.-C. Kilhoffer, *Top. Fluoresc. Spectrosc.*, 2000, **6**, 175-209.
57. M. Y. Liu, T. Y. Chen, B. Ahamed, J. Li and K. W. Yau, *Science*, 1994, **266**, 1348-1354.
58. M. J. Tucker, R. Oyola and F. Gai, *J. Phys. Chem. B*, 2005, **109**, 4788-4795.
59. M. A. Shalaby, C. W. Grote and H. Rapoport, *J. Org. Chem.*, 1996, **61**, 9045-9048.
60. S. Batjargal, Y. Huang, Y. Wang and E. J. Petersson, *J. Peptide Sci.*, 2014, **20**, 87-91.
61. P. E. Dawson, T. W. Muir, I. Clarklewis and S. B. H. Kent, *Science*, 1994, **266**, 776-779.
62. T. Tanaka, A. M. Wagner, J. B. Warner, Y. X. J. Wang and E. J. Petersson, *Angew. Chem. Int. Ed.*, 2013, **52**, 6210-6213.
63. L. Wang and P. G. Schultz, *Angew. Chem. Int. Ed.*, 2005, **44**, 34-66.
64. R. F. Wissner, S. Batjargal, C. M. Fadzen and E. J. Petersson, *J. Am. Chem. Soc.*, 2013, **135**, 6529-6540.
65. R. F. Wissner, A. M. Wagner, J. B. Warner and E. J. Petersson, *Synlett*, 2013, **24**, 2454-2458.
66. C. J. McKnight, D. S. Doering, P. T. Matsudaira and P. S. Kim, *J. Mol. Biol.*, 1996, **260**, 126-134.
67. C. J. McKnight, P. T. Matsudaira and P. S. Kim, *Nat. Struct. Biol.*, 1997, **4**, 180-184.
68. J. M. Goldberg, X. S. Chen, N. Meinhardt, D. C. Greenbaum and E. J. Petersson, *J. Am. Chem. Soc.*, 2014, **136**, 2086-2093.